

**1.**

① The wear volume ( $V$ ) calculation equation:

$$V=(m_1-m_2)/\rho \quad \text{Equation (1-1)}$$

$m_1$  —The quality of the sample before test, unit: g;

---

$m_2$  —The quality of the samples after test, unit: g;

$\rho$  —The density of the sample in the test temperatures, unit: g/mm<sup>3</sup>.

②The volume wear rate ( $\omega$ ) calculation equation:

$$\omega=V/(F \times L)[\text{mm}^3/(\text{Nm})] \quad \text{Equation (1-2)}$$

$V$  — Wear volume, unit: mm<sup>3</sup>

$L$  — Sliding distance, unit: m;

$F$  — Loading, unit: N.

2.

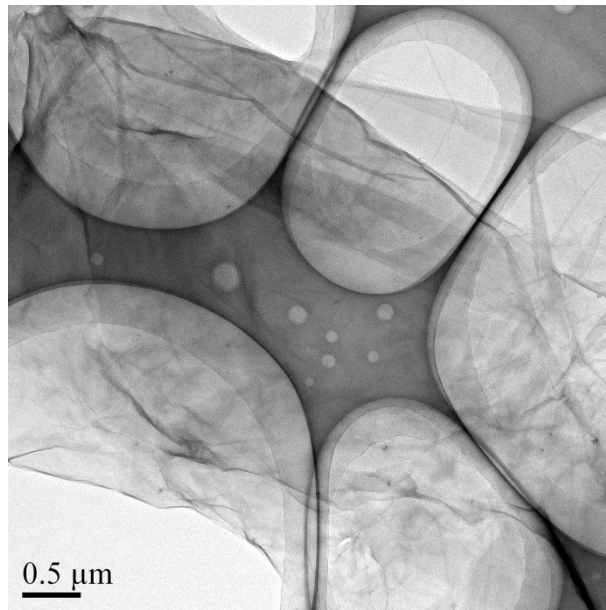


**Fig. S1 TEM image of GO.**

As shown in Fig. S1, the morphologies and structures of the GO was investigated by TEM. The obtained GO sample is transparent and has a crumpled and rippled structure.

3.

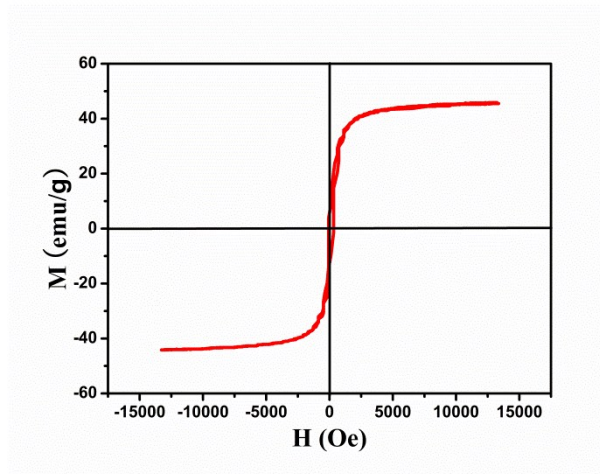


**Fig. S2 Magnetization curve of GNS-Fe<sub>3</sub>O<sub>4</sub> composite at room temperature.**

The field dependence of magnetization for the GNS-Fe<sub>3</sub>O<sub>4</sub> composite was measured at room temperature by VSM, as shown in Fig. S2. The saturation magnetization ( $M_s$ ) is 45.8 emu/g for the GNS-Fe<sub>3</sub>O<sub>4</sub> composite. The magnetization hysteresis loops of GNS-Fe<sub>3</sub>O<sub>4</sub> composite shows S-like, which is typical superparamagnetic material because of its high  $M_s$ .

4.

**Table S1 The impact strength of the composites with different content of GNS.**

Content of GNS (wt%)	Sample 1	Sample 2	Sample 3	Sample 4	Sample 5	Average Value
0	13.61	12.87	14.13	13.08	14.51	13.64
0.2	14.42	13.67	13.89	14.86	15.01	14.37
0.4	16.33	15.31	15.74	16.01	16.25	15.93
0.6	15.79	16.45	15.99	16.87	16.76	16.37
0.8	14.98	16.01	16.69	15.88	16.74	16.06
1	13.72	14.98	14.2	14.77	14.75	14.48

**Table S2 The impact strength of the composites with different content of GNS-Fe<sub>3</sub>O<sub>4</sub>.**

Content of GNS-Fe <sub>3</sub> O <sub>4</sub> (wt%)	Sample 1	Sample 2	Sample 3	Sample 4	Sample 5	Average Value
0	13.61	12.87	14.13	13.08	14.51	13.64
0.2	14.59	13.68	15.21	15.69	13.18	14.47
0.4	14.68	16.71	15.09	15.48	14.66	15.32
0.6	14.87	16.32	16.39	15.07	15.53	15.64
0.8	15.86	14.28	14.08	15.17	14.41	14.76
1	11.96	14.28	13.82	12.66	14.68	13.48

5.

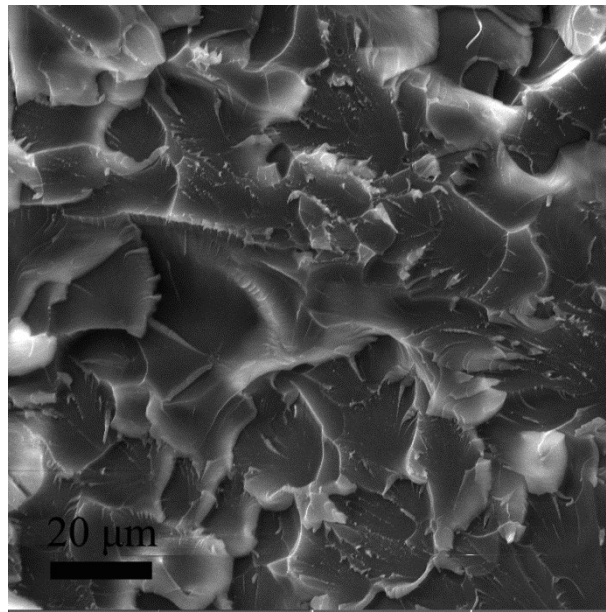


**Fig. S3 SEM image of the fracture surface of 0.6 wt%GNS/BMI.**

Fig. S3 shows the fracture surface of 0.6 wt%GNS/BMI composites. The large roughness of the cracked composite surface shows stronger filler-matrix interfacial interactions, indicating strong filler-matrix interfacial interactions. In addition, the composites show a good dispersion and homogeneity of GNS, and there is almost no GNS restacks in GNS/BMI composites.

6.

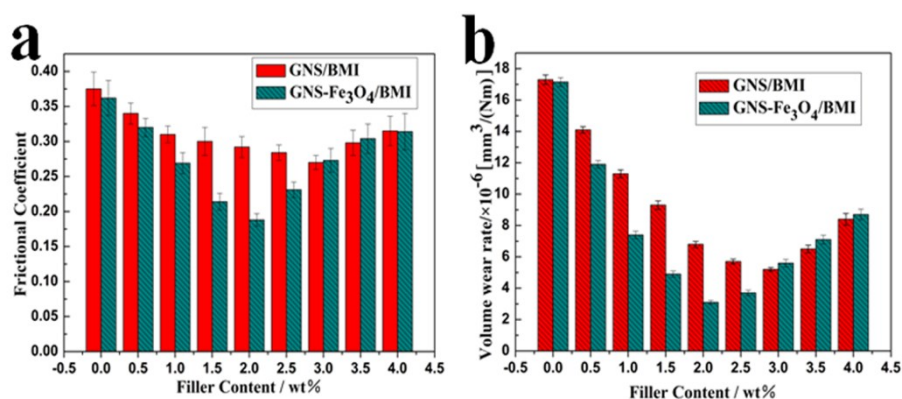


**Fig. S4 Tribological properties of GNS/BMI and GNS-Fe<sub>3</sub>O<sub>4</sub>/BMI composites with different filler content. (a) Frictional coefficient, (b) Wear rate.**

To confirm the synergy exist between GNS and Fe<sub>3</sub>O<sub>4</sub> nanorods in improving the tribological property of BMI resin and the horizontal alignment is conducive to fully demonstrate the outstanding performance of GNS, the GNS/BMI and GNS-Fe<sub>3</sub>O<sub>4</sub>/BMI were prepared without alignment treatment and the tribological properties of GNS/BMI and GNS-Fe<sub>3</sub>O<sub>4</sub>/BMI were studied separately. As we all know, the tribological properties of GNS is better than Fe<sub>3</sub>O<sub>4</sub> nanoparticles, and therefore the tribological properties of Fe<sub>3</sub>O<sub>4</sub>/BMI composites do not study. It can be seen that the addition of GNS (or GNS-Fe<sub>3</sub>O<sub>4</sub>) has certain influence on the friction and wear properties of GNS/BMI (or GNS-Fe<sub>3</sub>O<sub>4</sub>/BMI) composites. The tendency of wear property changes with different amount of GNS (or GNS-Fe<sub>3</sub>O<sub>4</sub>) is similar to the friction property of composites. The lowest frictional coefficient of the GNS/BMI composites is 0.27, and the lowest wear rate of the GNS/BMI composites is  $5.2 \times 10^{-6} \text{ mm}^3/(\text{N}\cdot\text{m})$ , when the content of GNS is 3.0 wt%. However, the lowest frictional coefficient of the GNS-Fe<sub>3</sub>O<sub>4</sub>/BMI composites is 0.19, and the lowest wear rate of the GNS-Fe<sub>3</sub>O<sub>4</sub>/BMI composites is  $3.1 \times 10^{-6} \text{ mm}^3/(\text{N}\cdot\text{m})$ , when the content of GNS-Fe<sub>3</sub>O<sub>4</sub> is merely 2.0 wt%. This result is mainly due to three reasons. Firstly, the self-restacking of the as-reduced graphene sheets can be prevented by loading the Fe<sub>3</sub>O<sub>4</sub> on the graphene surface.<sup>1</sup> Secondly, a more continuous and self-lubricating transfer film can be formed on the worn surface of counterpart steel ring and composites during the wear process after adding the Fe<sub>3</sub>O<sub>4</sub> nanorods. Thirdly, the migration rate of graphene sheets during the wear process can be improved by loading the larger sized Fe<sub>3</sub>O<sub>4</sub> nanorods on the graphene surface<sup>2</sup> because they can provide enough mechanical abrasion. When the fillers amount further increase, the tribological properties of composites decrease. This phenomenon can be explained that excessive GNS (or GNS-Fe<sub>3</sub>O<sub>4</sub>) agglomerate in the BMI resin and creating more micro-cracks in the composites under the high load, thus the mechanical properties of the composites decreased. With the decrease of the mechanical properties, the load-carrying capability of the composites decreased, thus the deformation of the composite will be increased during the friction test process. Consequently, the advantages of the GNS (or GNS-Fe<sub>3</sub>O<sub>4</sub>) can't be fully realized and the tribological properties of composites decrease when the fillers amount are excessive.

[1] G. Goncalves, P. Marques, C. M. Granadeiro, H. I. S. Nogueira, M. K. Singh, J. Gracio, *Chem. Mater.*, 2009, **21**, 4796-47802.

[2] F. Llie, *J. Nanopart. Res.*, 2013, **15**, 1-8.

7.

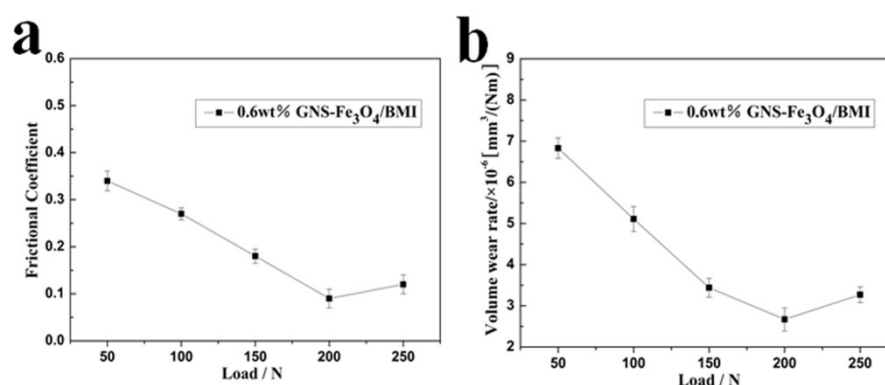


**Fig. S5 Tribological properties of aligned GNS-Fe<sub>3</sub>O<sub>4</sub>/BMI composites (0.6wt% GNS-Fe<sub>3</sub>O<sub>4</sub>) under different loads. (a) Coefficient of friction; (b) Wear rate.**

From Fig. S5a, it is obvious that the friction coefficients gradually decrease from 50 to 200 N with an increase in applied loads. It may be attributed to the fact that the better compaction and larger coverage of transfer layers are formed at higher applied loads, playing a dominant role in anti-wear properties.<sup>1</sup> While, the friction coefficients slightly increases at 250 N. It may be ascribed to the fact that at higher applied load of 250 N, the existing transfer layers get thickened and easily pelt off and clog between the rubbing surfaces, resulting in higher friction coefficient.

The wear rates are observed to decrease with increasing the applied load from 50 to 200 N and slightly increase there after beyond this applied load as evident from Fig. S5b. The slight increase in wear rates at higher applied load of 250 N may be ascribed to that the existing transfer layers maintain with difficulty and pelt off when the applied load is higher, resulting in the increase of wear rate.<sup>2,3</sup> The poor compatibility between GNS-Fe<sub>3</sub>O<sub>4</sub> and BMI resin is the main reason for this result.

[1] R. Tyagi, D. Xiong, J. Li, *Wear*, 2011, **270**, 423-430.

[2] C. S. Ramesh, A. Ahamed, *Wear*, 2011, **271**, 1928-1939.

[3] Z. Xu, X. Shi, Q. Zhang, W. Zhai, X. Li, J. Yao, Y. Xiao, *Tribol. Lett.* 2014, **55**, 393-404.

8.

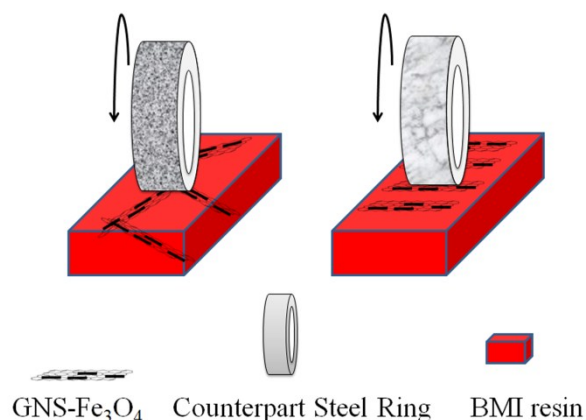


**Fig. S6 The friction mechanism simulation diagrams of GNS-Fe<sub>3</sub>O<sub>4</sub>/BMI composites (the left one) and aligned GNS-Fe<sub>3</sub>O<sub>4</sub>/BMI composites (the right one).**

To further illustrate the working mechanism of GNS-Fe<sub>3</sub>O<sub>4</sub> and the advantages of aligned GNS-Fe<sub>3</sub>O<sub>4</sub> in friction tests, we provide the illustration of working mechanism of GNS-Fe<sub>3</sub>O<sub>4</sub> (Fig. S6). It can be seen clearly that a larger volume fraction of GNS-Fe<sub>3</sub>O<sub>4</sub> distribution near the aligned GNS-Fe<sub>3</sub>O<sub>4</sub>/BMI composites surface compared to the GNS-Fe<sub>3</sub>O<sub>4</sub>/BMI composites with the same addition. During the wear process of the GNS-Fe<sub>3</sub>O<sub>4</sub>/BMI composite, the GNS-Fe<sub>3</sub>O<sub>4</sub> and the resin can be precipitated, then rough and discontinuous thin “carbon film” containing GNS-Fe<sub>3</sub>O<sub>4</sub> and the BMI resin forms on the surface of counterpart steel ring. Compared to GNS-Fe<sub>3</sub>O<sub>4</sub>/BMI composites, the more GNS-Fe<sub>3</sub>O<sub>4</sub> particles in the aligned GNS-Fe<sub>3</sub>O<sub>4</sub>/BMI composites can be precipitated, then more uniform and lubricating thinner “carbon film” containing GNS-Fe<sub>3</sub>O<sub>4</sub> forms on the surface of counterpart steel ring during the wear process of the composite. With the formation of the uniform and lubricating thinner “carbon film”, sliding occurs between the surface of the composite block and the “carbon film” other than between the rough surface of the composite and the steel counterpart.



9.

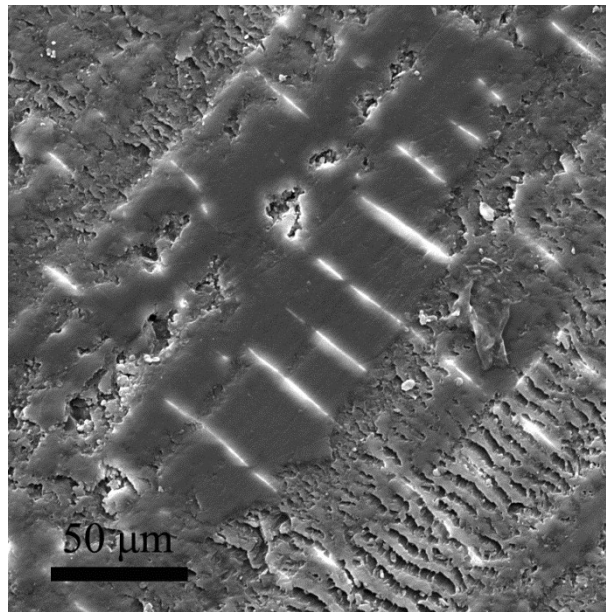


**Fig. S7 SEM image of worn surfaces taken from the composites with 0.6 wt% GNS-Fe<sub>3</sub>O<sub>4</sub> (the bottom surface) in wear test.**

The SEM image of worn surfaces was taken from the composites with 0.6 wt% GNS-Fe<sub>3</sub>O<sub>4</sub> (the bottom surface) in wear test. Obvious cracks and plate-like flake away can be seen on the wear surface of GNS-Fe<sub>3</sub>O<sub>4</sub>/BMI composite (Fig. S7), which is the characteristic of adhesive wear mechanism. This indicates that the wear resistance of BMI is poor in sliding against the steel ring.

10.

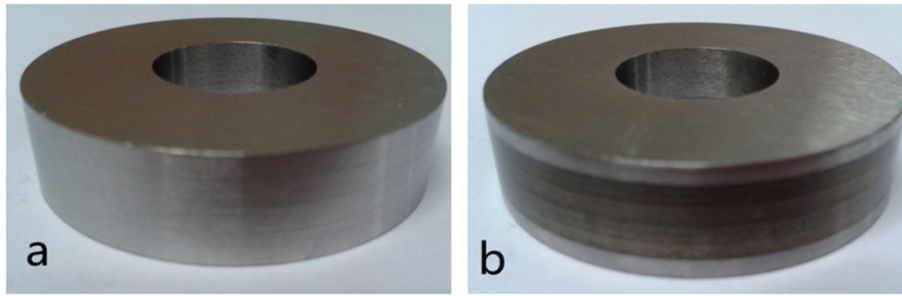


**Fig. S8 Digital photos of counterpart steel ring friction before (a) and after (b) the friction test of GNS-Fe<sub>3</sub>O<sub>4</sub>/BMI composites.**

It can be seen that thin film is formed on the counterpart steel ring surface after the friction test, which is attributed to the fact that the aligned GNS-Fe<sub>3</sub>O<sub>4</sub> in the matrix near the surface is exposed and act as the lubricating thin “carbon film” on the counterpart steel ring surface.

11.

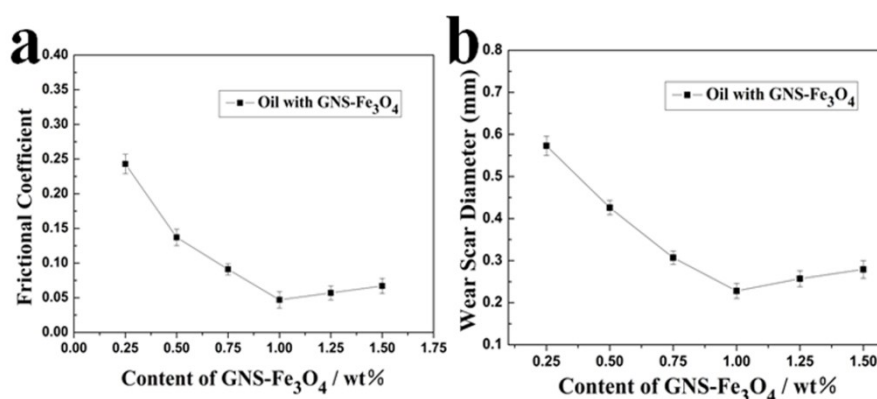


**Fig. S9 Tribological properties of GNS-Fe<sub>3</sub>O<sub>4</sub> based paraffin oil. (a) Coefficient of friction, (b) Wear scar diameter.**

As-prepared GNS-Fe<sub>3</sub>O<sub>4</sub> composites were distributed into paraffin base oil by 30 min ultrasonication, and then a series of suspended oil samples were obtained. Tribological properties of the oil mixed with GNS-Fe<sub>3</sub>O<sub>4</sub> composites were investigated using a universal micro-tribotester (UMT-2, Center for Tribology Inc., USA) at a rotating speed of 1450 rpm and load of 500 N, for 10 min. The wear scar diameters (WSD) on the steel balls were measured using an optical microscope to an accuracy of  $\pm 0.01$  mm. At least three tests, with standard deviations lower than 10%, were performed under the same experimental conditions for each sample. Fig. S9a shows variations of the friction coefficient with the content of GNS-Fe<sub>3</sub>O<sub>4</sub>. It is obvious that with the increase in the content of GNS-Fe<sub>3</sub>O<sub>4</sub>, the friction coefficient reduces rapidly. Fig. S9b shows the relationship between the content of GNS-Fe<sub>3</sub>O<sub>4</sub> and WSD. Seen from the curve, GNS-Fe<sub>3</sub>O<sub>4</sub> resulted in the improvement of anti-wear properties of the base oil. The reduction in friction coefficient implies that GNS-Fe<sub>3</sub>O<sub>4</sub> composites can serve as spacers, preventing the rough contact between counterparts, thereby improving the tribological property of base lubricant considerably. However, when the content of GNS-Fe<sub>3</sub>O<sub>4</sub> is more than 1.0 wt%, the frictional coefficient of composites increases slightly. This phenomenon can be explained that excessive GNS-Fe<sub>3</sub>O<sub>4</sub> agglomerate in the oil and making greater resistance under the high loading, thus the advantages of the GNS-Fe<sub>3</sub>O<sub>4</sub> can't be fully realized and the friction coefficient of composites increases.

12.

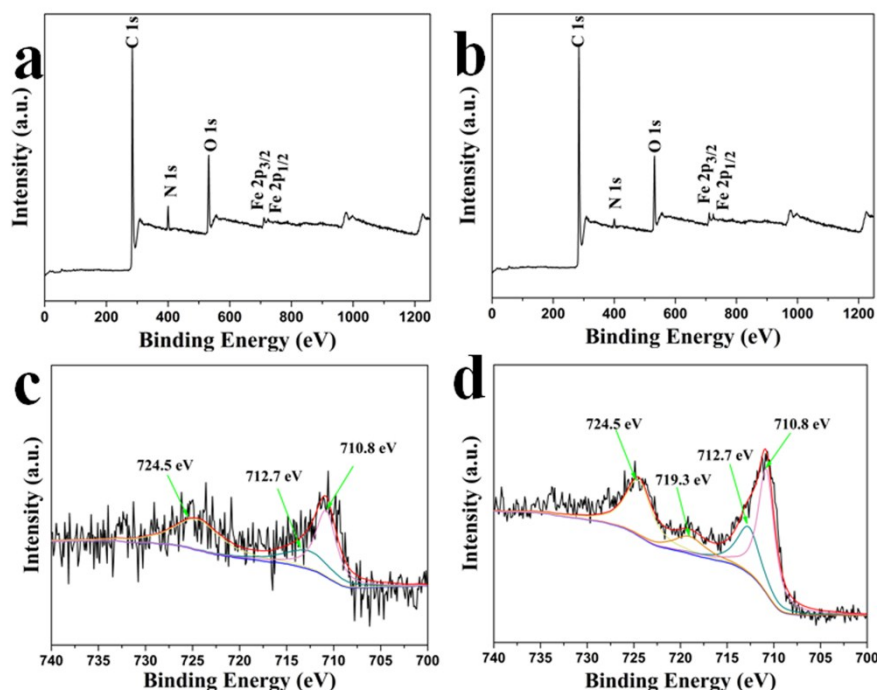


**Fig. S10 XPS spectrum of aligned GNS-Fe<sub>3</sub>O<sub>4</sub>/BMI composites (1.0 wt%): wide scan of the composites before (a) and after (b)friction testing; (c) Fe 2p of the composites before (c) and after (d) friction testing.**

The worn surfaces of the composites with aligned GNS-Fe<sub>3</sub>O<sub>4</sub> (1.0 wt%) before friction testing and after friction testing were analyzed by XPS for acquiring more information about the tribochemical reactions during sliding. The Fe2p peak of the composites with aligned GNS-Fe<sub>3</sub>O<sub>4</sub> before testing is very weak, which is mainly attributed to the content of Fe<sub>3</sub>O<sub>4</sub> is rare and the Fe<sub>3</sub>O<sub>4</sub> is coated with BMI resin. The Fe 2p spectrum simulation peaks at 712.7, 724.5, and 710.8 eV characterized Fe<sub>3</sub>O<sub>4</sub> (Fig. 4d).<sup>1</sup> Compared to the Fe2p peak of the composite before testing, the Fe 2p peak of the composite after testing is strong, which may be due to the fact that the Fe<sub>3</sub>O<sub>4</sub> in the composites near the surface is exposed and distributed to the surface of the composites or the counterpart steel ring during wear process. In the Fe 2p spectrum simulation peaks, a new peak emerges at 719.3 eV, which is assigned to the Fe<sup>3+</sup> of the  $\alpha$ -Fe<sub>2</sub>O<sub>3</sub>.<sup>2</sup> This may be due to the fact that the Fe<sub>3</sub>O<sub>4</sub> is oxidized to  $\alpha$ -Fe<sub>2</sub>O<sub>3</sub> during the wear process.

**Table S3 The atomic concentration of elements on the worn surface of the composites with aligned GNS-Fe<sub>3</sub>O<sub>4</sub> (1.0 wt%) before and after friction testing.**

Composites	Atomic concentration			
	C	O	N	Fe
Before	79.19	15.61	4.15	1.05
After	87.13	8.21	1.32	3.34

To collect more information of the tribochemical reactions, the atomic concentrations of elements on the worn surface of the composites with aligned GNS-Fe<sub>3</sub>O<sub>4</sub> (1.0 wt%) before and after testing are shown in Table S3. Obviously, the atomic concentration of C on the worn surface of the composites

with aligned GNS-Fe<sub>3</sub>O<sub>4</sub> (1.0 wt%) after testing is 87.13%, higher than the composites before testing. The atomic concentration of N is also shown a significant decrease. This may be due to the fact that the aligned GNS-Fe<sub>3</sub>O<sub>4</sub> in the composites near the surface is exposed and inhibited the transfer of resin to the surface of the sample and the counterpart steel ring during the wear process, thereby improving the anti-friction and anti-wear capacity of the resin composites.

[1] R. Chen, L. Chai, Q. Li, Y. Shi, Y. Wang, A. Mohammad, *Environ. Sci. Pollut. R.*, 2013, **20**, 7175-7185.

[2] H. J. Song, X. H. Jia, N. Li, X. F. Yang, H. Tang, *J. Mater. Chem.*, 2012, **22**, 895-902.

13.

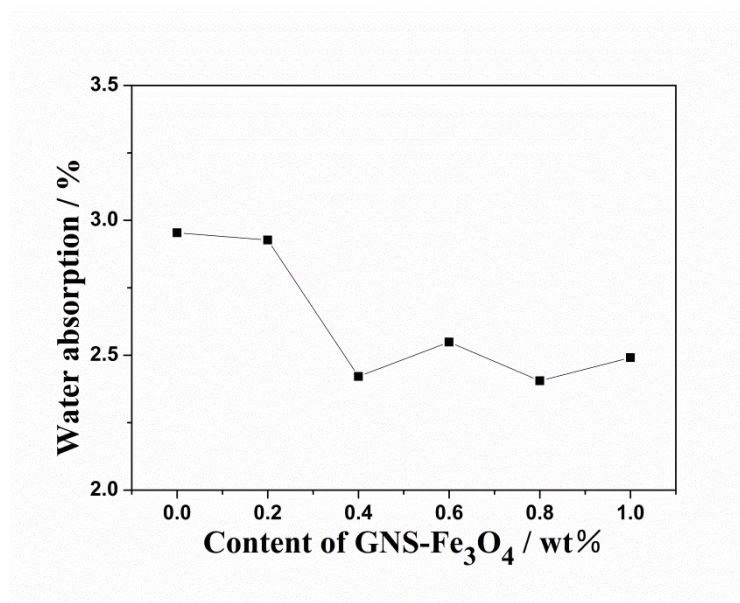


**Fig. S11** The water absorption of the composites with different content GNS-Fe<sub>3</sub>O<sub>4</sub>.

The water absorption of the composites with different content of GNS-Fe<sub>3</sub>O<sub>4</sub> is shown in Fig. S11. It can be seen that suitable amount of GNS-Fe<sub>3</sub>O<sub>4</sub> can properly reduce the water absorption of BMI resin, which is mainly attributed to the sheet structure of graphene and the hydrophobicity of graphene and Fe<sub>3</sub>O<sub>4</sub>.